30 April 1999

ELSEVIER

Chemical Physics Letters 304 (1999) 155–166

CHEMICAL PHYSICS LETTERS

Pathways for photoinduced electron transfer in *meso*-nitro-phenyl-octaethylporphyrins and their chemical dimers

Valentine Knyukshto, Eduard Zenkevich *, Evgenii Sagun, Alexander Shulga, Sergei Bachilo

Institute of Molecular and Atomic Physics, Academy of Sciences of Belarus, 70 F. Skaryna Ave., 220 072 Minsk, Belarus

Received 20 October 1998; accepted 11 March 1999

Abstract

The photophysical properties of *meso*-nitro-phenyl-octaethylporphyrins and their dimers with electron-accepting NO_2 groups in the *para*-, *meta*- and *ortho*-positions of the phenyl ring were studied. For the *ortho*-NO_2 case in deaerated toluene at 295 K, strong fluorescence quenching is caused by the intramolecular electron transfer from the porphyrin S_1 state in the absence of phenyl ring librations around the single C–C bond ('normal' region, non-adiabatic case). T_1 state lifetime shortening for the same compounds is explained by thermally activated transitions to upper-lying charge-transfer states of the radical ion pair as well as by the rise of the intersystem crossing $T_1 \rightsquigarrow S_0$ rate constants caused by T_1 states mixing with charge-transfer states.

1. Introduction

Stimulated by biophysical studies of the structure of photosynthetic reaction centres in vivo [1], numerous synthetic models have advanced considerably during the past decade, especially those based on porphyrin or chlorophyll subunits covalently linked to electron acceptors by various spacers, mimicking vectorial electron transfer (ET) processes [2–8]. It has been shown that intracomplex ET has a wide (up to fs) time-scale range, being dependent on the energetic and redox properties of the interacting donor–acceptor (D–A) components, their mutual geometry and the D–A intercenter distance, the temperature and polarity of the solvent, as well as on the nature of the spacer.

In this relation, it follows from literature data that the use of an NO_2 group as an electron acceptor did not seem to be promising enough because of the relatively small ET rate constants with respect to those obtained for numerous synthetic porphyrin–quinone D–A pairs [3,4,9]. Strategies used for linking the porphyrin macrocycle and the NO_2 group included the following systems: (1) octaethylporphyrins with *meso*-NO_2 groups [10,11]; (2) tetraphenylporphyrins, **TPP**, [12] and tetraazaporphyrins [13] with β-nitro groups; and (3) tetraphenylporphyrins with NO_2 groups in the *ortho*- and *para*-positions of the phenyl ring [14]. In general, on the basis of the results obtained in Refs. [10–14], one may conclude that at room temperature in non-polar

* Corresponding author. E-mail: zenkev@imaph.bas-net.by

0009-2614/99/$ - see front matter
PII: S0009-2614(99)00323-1

solvents, the fluorescence quenching is due to photoinduced ET with rate constants in the range of $k_{et}^{S} = (1–5) \times 10^{8}\ s^{-1}$ for all investigated porphyrins with covalently linked nitro groups (free bases and Zn complexes). This relatively small quenching compared with that for quinones may be attributed not only to the lesser electron accepting properties of the nitro group itself but to steric reasons which do not provide the optimal overlap of molecular orbitals for the porphyrin macrocycle and NO_2 group determining the electronic coupling term value for ET processes [15]. These factors in detail as well as the possible role of porphyrin triplet states in photoinduced ET processes are still unknown for nitroporphyrins.

In some cases, porphyrin–(electron or energy) acceptor systems [3–7,14,16] and multiporphyrin arrays with or without electron acceptors [8,9,17–20] contain an inserted phenyl spacer between the redox pair or between interacting tetrapyrrole macrocycles. Correspondingly, steric interactions of the phenyl spacer with the connected subunits as well as the π-electronic nature of the linkage may influence both the deactivation of porphyrin excited states and the electron/energy transfer efficiency. The specific role of steric interactions of *meso*-phenyls with β-CH_3 pyrrole substituents was mentioned for ET processes in carotenoid-porphyrin-quinone triads [7]. The results obtained in Ref. [16] show that the T–T energy transfer in carotene-porphyrin diads is mediated by a through-bond (superexchange) mechanism involving the π-electrons of the phenyl linkage. The theoretical model for the bridge-assisted, long-range ET was presented in Ref. [20], showing that even with modest dephasing rates the ET rates become distant independent. Recently, we have found a strong decrease of triplet lifetimes (by ~ 300–500 times in degassed toluene at 295 K) for mono- and di-*meso*-phenyl substituted octaethylporphyrins, while spectral-kinetic parameters of S_0 and S_1 states remain unchanged [21]. This quenching was attributed to the porphyrin non-planar dynamic distortions in the excited T_1 states, caused by internal librations of the phenyl ring around the single meso C–C bond and the interaction of the phenyl ring with the π-conjugated macrocycle.

To understand the influence of the steric properties of the *meso*-phenyl spacer and its π-electron system on the ET pathways and efficiency better, we have prepared a series of *meso*-phenyl substituted octaethylporphyrins and their chemical phenyl coupled dimers, containing covalently linked one or two NO_2 groups in the *para*-, *meta*- and *ortho*-positions of the phenyl spacer (Fig. 1). Here we present the results of steady-state and time-resolved comparative studies of the S_1 and T_1 states deactivation for these compounds and the corresponding analogs not having nitro groups.

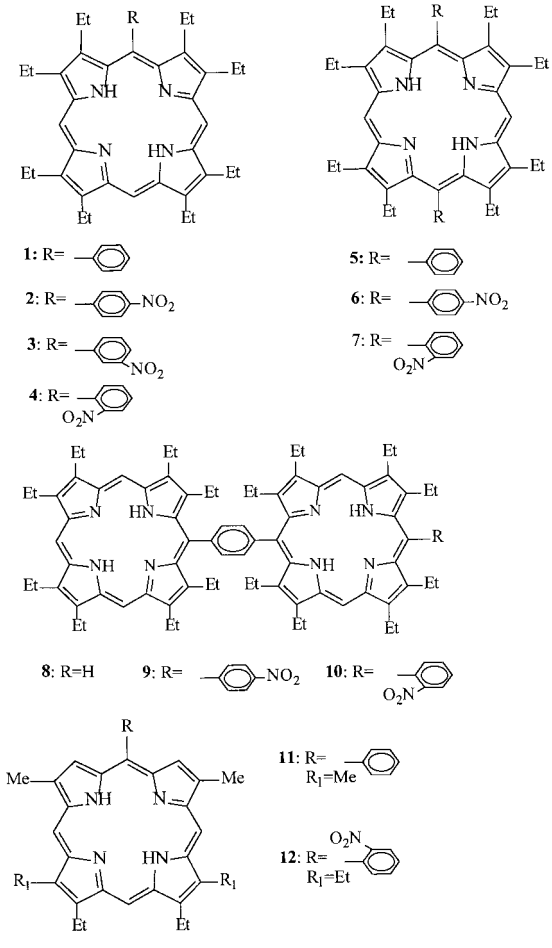

Fig. 1. Chemical structures of the investigated compounds. **1** = OEP-Ph; **2** = OEP-Ph(*p*-NO_2); **3** = OEP-Ph(*m*-NO_2); **4** = OEP-Ph(*o*-NO_2); **5** = Ph-OEP-Ph; **6** = (*p*-NO_2)Ph-OEP-Ph(*p*-NO_2); **7** = (*o*-NO_2)Ph-OEP-Ph(*o*-NO_2); **8** = OEP-Ph-OEP; **9** = OEP-Ph-OEP-Ph(*p*-NO_2); **10** = OEP-Ph-OEP-Ph(*o*-NO_2); **11** = TMDE-Ph; **12** = TEDM-Ph(*o*-NO_2).

2. Experimental

5-*Meso*-phenyl substituted compounds, octaethylporphyrin **OEP-Ph** and the corresponding nitroporphyrins **OEP-Ph(*p*-NO_2)**, **OEP-Ph(*m*-NO_2)** and **OEP-Ph(*o*-NO_2)**, were synthesised and purified according to the method described in Ref. [22]. The same procedure was used for the preparation and characterisation of 5-*meso*-phenyl substituted tetramethyldiethylporphyrin **TMDE-Ph** and 5-*meso-ortho*-nitro-phenyl substituted tetraethyldimethylporphyrin **TEDM-Ph(*o*-NO_2)**. The synthesis of 5,15-diphenyl substituted **OEP** molecules, **Ph-OEP-Ph**, **(*p*-NO_2)-Ph-OEP-Ph(*p*-NO_2)** and **(*o*-NO_2)Ph-OEP-Ph(*o*-NO_2)**, was carried out on the basis of the methods described in Refs. [23,24]. The porphyrin chemical dimers **OEP-Ph-OEP**, **OEP-Ph-OEP-Ph(*p*-NO_2)** and **OEP-Ph-OEP-Ph(*o*-NO_2)**, were synthesised according to known methods [17–19]. The corresponding compounds with one or two NO_2 groups were synthesised on the basis of the methods cited above.

All spectroscopic experiments, S_1 and T_1 states decay measurements, as well as the determination of singlet oxygen generation quantum yields were performed using commercial and hand-made laboratory equipment described in Refs. [25,26]. When studying T_1 states parameters in liquid solutions at 295 K, porphyrin concentrations of $\sim 10^{-6}$ M were used for the T–T annihilation diminishing. Most results at 295 K were obtained in toluene (Spectroscopic Grade) unless otherwise noted. Methylcyclohexane–toluene (6:1) glassy rigid matrices were used at 77 K. In order to study the excited states quenching by dissolved oxygen, the comparative kinetic measurements were carried out in deaerated samples (5–7 freeze–pump–thaw cycles, purging down to 10^{-5} Torr pressure). All experiments for every sample were completed within 1–2 h following preparation.

3. Results and discussion

3.1. Spectral properties

At 295 K in toluene, absorption and fluorescence spectra of *para*- and *meta*-nitro substituted porphyrins remain practically the same with respect to those for the corresponding *meso*-phenyl substituted compounds without nitro groups (Table 1). In the case of the *ortho*-NO_2 substitution, the Stokes shift remains the same but the electronic spectra are slightly red-shifted by $\Delta\lambda \sim 1$–6 nm. In addition, a relative decrease of the $Q(0,0)$ bands intensities both in fluorescence and absorption spectra with respect to the corresponding intensities of vibronic $Q(1,0)$

Table 1
Absorption and emission parameters at room temperature and low temperatures

No.	Compound	Absorpt. A^{soret} (nm) 295 K	Absorpt. λ^{Soret} (nm) 77 K	Absorpt. λ_{0-0} (nm) 295 K	Fluoresc. λ_{0-0} (nm) 295 K	Absorpt. λ_{0-0} (nm) 77 K	Fluoresc. λ_{0-0} (nm) 77 K	Phosph. λ_{0-0} (nm) 77 K	$\Delta E(S_1-T_1)$ (cm^{-1}) 77 K
1	**OEP-Ph**	403	402	626	628	620	621	790	3450
2	**OEP-Ph(*p*-NO_2)**	403	405	627	628	620	621	790	3450
3	**OEP-Ph(*m*-NO_2)**	403	405	628	630	621	622	792	3470
4	**OEP-Ph(*o*-NO_2)**	404	405	629	634	623	624	797	3490
5	**Ph-OEP-Ph**	411	411	629	633	623	624	806	3620
6	**(*p*-NO_2)Ph-OEP-Ph(*p*-NO_2)**	412	411	631	635	625	626	795	3400
7	**(*o*-NO_2)Ph-OEP-Ph(*o*-NO_2)**	410	412	635	639	627	628	815	3650
8	**OEP-Ph-OEP**	413	410	625	626	625	626	803	3520
9	**OEP-Ph-OEP-Ph(*p*-NO_2)**	418	413	631	638	623	625	810	3650
10	**OEP-Ph-OEP-Ph(*o*-NO_2)**	419	413	632	640	626	628	815	3650
11	**TMDE-Ph**	403	402	627	630	622	623	796	3490
12	**TEDM-Ph(*o*-NO_2).**	403	404	630	635	624	625	801	3520

Experimental data at 295 K were obtained in toluene; at 77 K a glassy matrix of methylcyclohexane–toluene mixture (6:1) was used. $\Delta E(S_1-T_1)$ is the energy gap between locally excited S_1 and T_1 states.

bands was observed followed by a half-width increase (by ~ 1.5 times) of the pure electronic transition bands (Fig. 2). Similar tendencies have been observed for 5-nitrooctaethylporphyrins [10], β-nitro-tetra-*para*-tolylporphyrins [12] and **TPP** with four NO_2 groups in *ortho*- and *para*-positions [14]. These spectral changes have been connected with the well-known fact that electron withdrawing substituents on the periphery of the porphyrin cause shifts to longer wavelength of the visible and Soret bands [12]. Table 1 shows that spectral properties of the **OEP-Ph-OEP** dimer are scarcely affected by nitro substitution.

Fig. 3 compares the transient triplet–triplet absorption spectra in the near IR region of *ortho*- and *para*-nitro substituted **OEP-Ph** molecules with those

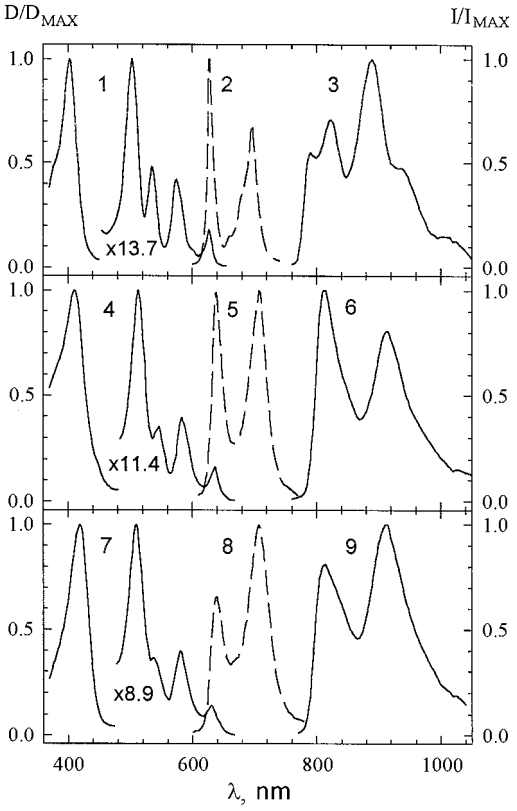

Fig. 2. Absorption (1, 4, 7) and fluorescence (2, 5, 8) spectra in toluene at 295 K and phosphorescence spectra (3, 6, 9) in methylcyclohexane–toluene mixture (6:1) at 77 K: **OEP-Ph** (1, 2, 3); **(*o*-NO_2)Ph-OEP-Ph(*o*-NO_2)** (4, 5, 6); and **OEP-Ph-OEP-Ph(*o*-NO_2)** (7, 8, 9).

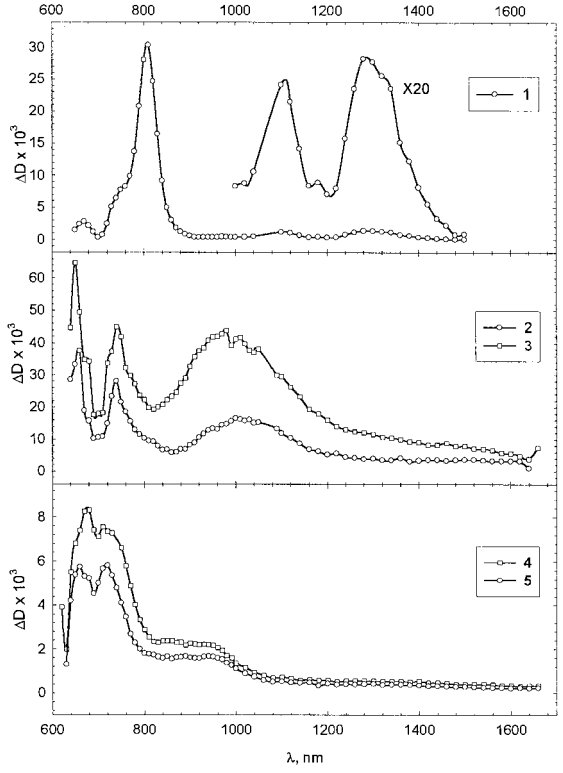

Fig. 3. Transient triplet–triplet absorption spectra (optical densities ΔD) following a 25 ns laser flash excitation of **OEP-Ph (*o*-NO_2)** (1), **OEP-Ph (*p*-NO_2)** (2), **OEP-Ph** (3), **OEP-Ph (*o*-CH_3)** (4) and **OEP** (5) under the same experimental conditions (deaerated toluene solution at 295 K, $\lambda_{exc} = 532$ nm).

of the corresponding compounds without nitro groups. According to our previous results [21], the noticeable difference between the T–T absorption spectra of **OEP** and **OEP-Ph** (Fig. 3, curves 5 and 3) may be connected with the non-planar conformational dynamics of **OEP-Ph** in the T_1 state due to internal librations of the phenyl ring around the single C–C bond. In such a situation, the energies of higher excited triplet states and extinction coefficients may differ for the compounds of these two types. It can be seen from Fig. 3 that T–T absorption spectra are partially the same for **OEP-Ph(*p*-NO_2)** and **OEP-Ph**, being somewhat red-shifted for the nitroporphyrin relative to those of **OEP-Ph** (Fig. 3, curves 2 and 3). The spectral similarity in this case is explained by the fact [21] that the presence of bulky substituents in the *para*- or *meta*-positions of the

phenyl ring in molecules of the **OEP-Ph** type does not influence their T_1 state characteristics relative to those of **OEP-Ph**. In the *ortho*-phenyl substituted **OEP-Ph(*o*-CH_3)** molecule containing a bulky CH_3 group, the non-planar dynamic conformations of the porphyrin macrocycle do not result in the locally excited T_1 state [21], and its T–T absorption spectrum practically coincides with that of a planar **OEP** molecule (Fig. 3, curves 4 and 5). In this relation, the transient T–T spectrum for **OEP-Ph(*o*-NO_2)** differs strikingly from those for both **OEP-Ph(*o*-CH_3)** and parent **OEP** molecules (Fig. 3, curves 1, 4 and 5). In addition, the relative intensities of **OEP-Ph(*o*-NO_2)** T–T absorption bands show a noticeable dependence on the solvent polarity. This means that locally excited T_1 states of nitro-phenyl substituted octaethylporphyrins are sensitive to the localisation of the NO_2 group and their deactivation and spectral properties are thought to be connected with ET reactions.

3.2. Photophysics and photochemistry

The main photophysical parameters for *meso*-nitro-phenyl substituted compounds as well as for the corresponding analogs without NO_2 groups are collected in Table 2. On the basis of these data and structural properties of the compounds **1**–**12** (Fig. 1) the following findings were revealed:

(1) At 295 K in degassed toluene, fluorescence quantum yields (φ_F^0) and lifetimes (τ_S^0) for *para*- and *meta*-NO_2 containing **OEP-Ph** molecules and their dimer **OEP-Ph-OEP** do not differ strikingly from those for the corresponding compounds which lack nitro groups. A small fluorescence quenching is still observed with rate constants of $k_{et}^S = 1.2 \times 10^6$–$1.0 \times 10^7\ s^{-1} < 1/\tau_S^0$, where τ_S^0 corresponds to the S_1 state decay of **OEP** type compounds without NO_2 groups. A minimal fluorescence quenching was found for the *meta*-NO_2 substitution in comparison with the *para*-NO_2 case. In addition, for *para*- and *meta*-NO_2-phenyl substituted **OEPs** a noticeable decrease of T_1 state lifetimes (τ_T^0) is observed, and the τ_T^0 shortening for **OEP-Ph(*m*-NO_2)** is smaller relative to that of **OEP-Ph(*p*-NO_2)**. For **OEP-Ph(*p*-NO_2)**, the τ_T^0 value is reduced by 2.1 times relative to that for **OEP-Ph**. The existence of the second nitro group in **(*p*-NO_2)Ph-OEP-Ph(*p*-NO_2)** leads to a shortening of τ_T^0 by 5.5 times with respect to $\tau_{TR}^0 = 16.5\ \mu s$ found for the parent **Ph-OEP-Ph** molecule. For the dimer **OEP-Ph-OEP(*p*-NO_2)**, T_1 state quenching is not observed with respect to τ_{TR}^0 value for **OEP-Ph-OEP**.

(2) For *ortho*-nitro-phenyl substituted **OEPs** and their dimers quantum yields φ_F decrease by 12–25 times and τ_S^0 shortening amounts to $\sim$100 times under same conditions, that is the rate constant of S_1 state quenching ranges up to the value of $k_{et}^S = 9.5 \times 10^9\ s^{-1}$. The observed S_1 state quenching is substantially greater than that found for numerous covalently linked porphyrin–NO_2 systems for which $k_{et}^S \leq (1\text{–}5) \times 10^8\ s^{-1}$ in non-polar solvents at room temperature [10–14].

Ortho-nitro-phenyl substituted **OEPs** and their dimers are also characterised by the essential enhancement of the non-radiative deactivation of T_1 states. For **OEP-Ph(*o*-NO_2)**, τ_T^0 decreases by 5.3 times with respect to the τ_T^0 value for **OEP-Ph**. In **(*o*-NO_2)Ph-OEP-Ph(*o*-NO_2)**, with two nitro groups in the opposite *meso*-phenyls, the τ_T^0 value is reduced by 33 times relative to that for **Ph-OEP-Ph**. In reality, τ_T^0 shortening in these nitroporphyrins ranges up to $\sim$1000–1500 times if one takes into account steric hindrance effects resulting in triplet long decays ($\tau_{TR}^0 \approx 700$–$750\ \mu s$) for the reference **OEP-Ph(*o*-CH_3)** molecule with the bulky *ortho*-phenyl substituent [21]. However, in the dimer **OEP-Ph-OEP-Ph(*o*-NO_2)** τ_T^0 shortening by $\sim$5 times relative to $\tau_{TR}^0 = 2.45\ \mu s$ of the parent **OEP-Ph-OEP** compound reflects the real T_1 state quenching. Actually, in the last case, torsion librations of the phenyl spacer around the single C–C bond and its interactions with two porphyrin subunits in **OEP-Ph-OEP** are not eliminated by the insertion of bulky substituents in the *ortho*-position at the second phenyl ring (see compounds **8** and **10**, Fig. 1). Fig. 4 shows that experimental points **4**, **7**, **10** for all *ortho*-nitro substituted compounds do not fit in the correlative dependence $\ln(k_T^0) = \ln(1/\tau_T^0) = f(\sum r^*)$ constructed on the basis of the influence of steric effects only.

(3) The enhanced nonradiative deactivation of excited states in nitroporphyrins manifests itself in their interaction with O_2 in toluene at 295 K. For the *para*- and *meta*-NO_2 case the second-order rate constants of S_1 state quenching by O_2 do not depend

Table 2
Photophysical and photochemical data in toluene at 295 K and in a glassy transparent matrix of methylcyclohexane–toluene mixture (6:1) at 77 K

Compound	τ_S (ns) 295 K	τ_S^0 (ns) 295 K	τ_S (ns) 77 K	φ_F [a] 295 K	φ_F 77 K	φ_P ($\times 10^4$) 77 K	τ_T (ms) 77 K	τ_T (ns) 295 K	τ_T^0 (s) 295 K	γ_T	γ_Δ	k_S [b] (10^9 M^{-1} s^{-1})	k_T [b] (10^9 M^{-1} s^{-1})	k_{et}^S [c] (s^{-1})	k_q^T [c] (s^{-1})
OEP-Ph	11.2	16.0	21.0	0.05	0.09	1.9	14.5	410	4.0	0.80	0.55	14.2	1.2		
OEP-Ph(p-NO_2)	10.7	15.4	21.3	0.05	0.06	1.5	13.5	710	1.9	–	0.3	15.8	0.5	2.4×10^6	2.8×10^5
OEP-Ph(m-NO_2)	11.5	15.7	–	0.07	0.09	3.0	16.9	470	3.0	–	–	12.9	1.0	1.2×10^6	8×10^5
OEP-Ph(o-NO_2)	0.105[d]	0.105	20.2	0.002	0.06	1.4	13.0	700	0.75	~ 0.1	< 0.01	–	–	9.5×10^9	1.3×10^6
Ph-OEP-Ph	9.9	13.0	–	0.05	0.06	0.9	10.3	380	16.5	–	–	13.4	1.4		
(p-NO_2)Ph-OEP-Ph(p-NO_2)	10.5	12.6	–	0.07	0.08	2.3	10.1	690	3.0	0.65	0.55	9.0	0.6	3.0×10^6	2.7×10^5
(o-NO_2)Ph-OEP-Ph(o-NO_2)	0.10[d]	0.10	16.0	0.001	0.07	1.6	11.0	400	0.5	~ 0.2	< 0.01	–	0.3	9.5×10^9	2.0×10^6
OEP-Ph-OEP	8.2	11.2	–	0.06	–	–	8.9	840	2.45	0.95	0.25	18.3	0.45		
OEP-Ph-OEP-Ph(p-NO_2)	7.8	10.1	15.0	0.04	0.07	1.7	8.2	865	2.4	–	0.3	15.8	0.4	1.0×10^7	$<1\times10^5$
OEP-Ph-OEP-Ph(o-NO_2)	0.3	0.3	16.0	0.005	0.04	0.9	8.2	450	0.5	–	< 0.01	–	–	3.2×10^9	1.6×10^6
TMDE-Ph	11.3	17.1	–	0.06	0.09	1.8	16	265	1640	0.80	0.80	16.7	2.1		
TEDM-Ph(o-NO_2)	1.7	1.7	–	0.01	0.07	2.2	12.9	315	195	–	–	–	1.8	5.0×10^8	4.5×10^3

All abbreviations and symbols are defined in the text.

[a] The rise of φ_F in degassed toluene solutions at 295 K(φ_F^0) is the practically same relative to that of τ_S.

[b] Second-order rate constants k_S and k_T for quenching of S_1 and T_1 states by O_2 were obtained using the Stern–Volmer equation $\tau^0/\tau = 1 + kC\tau^0$ (a), where τ^0 corresponds to S_1 or T_1 state decay in the absence of O_2, $C = 1.8\times10^{-3}$ M is the O_2 concentration in toluene at 295 K [11,27].

[c] Calculations of the rate constants of S_1 and T_1 states quenching for nitroporphyrins were carried out on the base of measured lifetimes using the well-known formula $k = 1/\tau^0 - 1/\tau_R^0$ (b), where τ_R^0 is the reference sample lifetime; in the case of T_1 state quenching the τ_{TR}^0 values corresponding to unquenched T_1 states were found to be 700–750 μs using the correlative dependence $\ln(k_T^0) = \ln(1/\tau_T^0) = f(\Sigma r^*)$ (Fig. 4) for compounds without *ortho*-NO_2 group but with the *ortho*-substituent characterized by the same overlap geometrical parameter $\Sigma r^* = 5.11$ Å.

[d] Decays were measured using the picosecond spectrometer, error = ±7%.

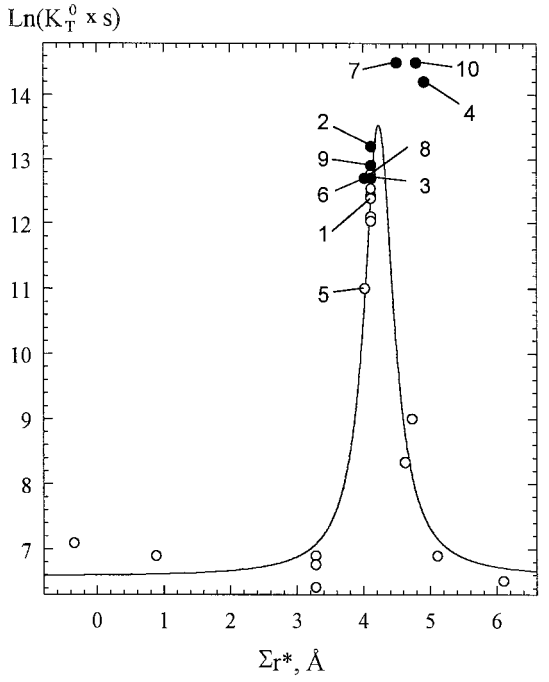

Fig. 4. The correlative dependence of the triplet state deactivation rate constants k_T^0 on the overlap geometrical parameter Σr^*, $\ln(k_T^0) = \ln(1/\tau_T^0) = f(\Sigma r^*)$, for octaalkylporphyrins and their dimers being studied in deoxygenated toluene at 295 K. Values of Σr^* were calculated using the formula $\Sigma r^* = (r_{w1}^x + r_{w2}^x) - d_x + (r_{w1}^y + r_{w2}^y) - d_y$ [21]. The effective van der Waals radii (r_w) values for interacting substituents were taken from a handbook of chemistry; intercenter distances (d_x, d_y) for these substituents were estimated for the hypothetical coplanar arrangement of the porphyrin and phenyl planes derived from the optimised structures of the compounds (HyperChem software, release 4, semiempirical methods AM1 and PM3) [21]. Experimental points ○ correspond to the triplet state deactivation rate constants k_T^0 for *meso*-phenyl substituted compounds without nitro group, investigated in details earlier [21]; experimental points ● were obtained for *meso*-nitrophenyl substituted octaethylporphyrins in this investigation. Numbers **1**–**10** correspond to compounds with the chemical structures shown in Fig. 1.

on the position of NO_2 group ($k_S = (1.3–1.6) \times 10^{10}$ M^{-1} s^{-1}) and are close to those for **OEP-Ph** and other **OEPs** without nitro groups. In the *ortho*-NO_2 case, we have not be able to estimate k_S values because of strong τ_S shortening. As for T_1 state quenching by O_2, a decrease of k_T values was observed for all *meso*-nitro-phenyl substituted **OEPs** relative to those for compounds which lack NO_2 groups. In *para*-nitro substituted compounds, the decrease of k_T values amounts to 1.5–2.5 times being the smallest one for the dimer **OEP-Ph-OEP-Ph(*p*-NO$_2$)**, while for *meta*-NO_2 substitution only a minor influence on k_T was found. In **(*o*-NO$_2$)Ph-OEP-Ph(*o*-NO$_2$)**, k_T is reduced by ~5 times.

The reduction of T_1 state lifetimes in *meso*-nitrophenyl substituted **OEPs** and their dimers leads to a pronounced decrease of quantum yields (γ_Δ) of the singlet oxygen $^1\Delta_g$ generation. For **OEP-Ph(*p*-NO$_2$)**, γ_Δ is reduced by 2 times relative to that of **OEP-Ph**. Because of a strong T_1 state shortening in the *ortho*-nitro case ($\tau_T^0 \approx 500–750$ ns), we have not be able to detect the singlet oxygen emission at normal atmospheric pressure directly. The low values of $k_T = 0.45 \times 10^9$ M^{-1} s^{-1} and $\gamma_\Delta = 0.25$ obtained for the dimer **OEP-Ph-OEP** may be connected with a possible increase of the dimer oxidation potential or with a rise of the bimolecular rate constant for the dissociation of the collision complex $[^3\text{Dimer} \cdots {}^3O_2] \rightarrow {}^3\text{Dimer} + {}^3O_2$ without T–T energy transfer and $^1\Delta_g$ formation [11].

(4) When transition from **TMDE-Ph** to **TEDM-Ph(*o*-NO$_2$)** (neither molecule has bulky C_2H_5 substituents at the β-pyrrolic positions neighbouring the phenyl ring, see Fig. 1, compounds **11** and **12**) the decrease of the τ_S^0 and τ_T^0 lifetimes is not so pronounced as that observed for the **OEP-Ph → OEP-Ph(*o*-NO$_2$)** case. For **TEDM-Ph(*o*-NO$_2$)**, the k_{et}^S value is less by ~20 times and the k_q^T is smaller by ~300 times relative to the corresponding parameters for **OEP-Ph(*o*-NO$_2$)**.

(5) The nonradiative deactivation of S_1 states for nitrooctaethylporphyrins is strongly enhanced in polar solvents (Table 3). At the same time, in glassy matrices at 77 K, the excited states quenching is fully absent for all the systems, and the main photophysical parameters for S_1 and T_1 states are fairly typical ones for planar porphyrins in low-temperature organic glasses [12,21,25].

If one takes into account the fact that *meso*-phenyl substitution in **OEPs** and their dimers does not change the nonradiative deactivation of the S_1 states [21] and absorption spectra are not perturbed by the nitro substitution (Fig. 2), the observed fluorescence quenching may be explained properly by ET processes from the porphyrin to the nitro group. As was mentioned above, the minimal quenching effect was observed for *meta*-NO_2 substitution with respect to

Table 3
Fluorescence parameters of *meso*-nitro-phenyl-octaethylporphyrins and their chemical dimers in solvents of various polarity (295 K, solutions at atmospheric pressure)

Compound	Toluene $\varepsilon = 2.379$ $n = 1.4969$		Acetone $\varepsilon = 20.7$ $n = 1.3586$		Acetonitrile $\varepsilon = 35.9$ $n = 1.3441$	
	φ_F	τ_S (ns)	φ_F	τ_S (ns)	φ_F	τ_S (ns)
OEP-Ph	0.05	11.2	–	–	0.06	11.3
OEP-Ph(*p*-NO_2)	0.05	10.7	0.015	–	0.002	~ 0.02[a]
OEP-Ph(*m*-NO_2)	0.07	11.5	0.02	3.7	0.003	0.6
OEP-Ph(*o*-NO_2)	0.002	0.105	–	–	0.001	~ 0.005[a]
(*p*-NO_2)Ph-OEP-Ph(*p*-NO_2)	0.07	10.5	0.03	–	0.005[b]	–
OEP-Ph-OEP-Ph(*p*-NO_2)	0.04	7.8	0.025	–	0.006[c]	–
TEDM -Ph(*o*-NO_2)	0.01	1.7	–	–	0.001	–

[a] Dimethylformamide ($\varepsilon = 36.7$; $n = 1.430$).
[b] Pyridine–acetonitrile mixture (1:10).
[c] Toluene–acetonitrile mixture (1:10).

that of the *para*-NO_2 case. The same tendency has been noticed for the T–T energy transfer in diads in which carotenoid was covalently linked to a **TPP** macrocycle at the *ortho*-, *meta*- and *para*-positions of a *meso* aromatic ring [16]. According to arguments presented in Ref. [16], it seems reasonable to suggest that the smallest quenching effect for the *meta*-NO_2 substitution in our case is due to the fact that for both the HOMO and the LUMO, the orbital density is greater at the *ortho*- and *para*-positions than it is at the *meta*-position of the phenyl spacer. Thus, the electronic coupling of the nitro group and the porphyrin, as mediated by the superexchange interaction [16], will also be greater at the *para*-position. In this relation, for **OEP-Ph(*m*-NO_2)** and **OEP-Ph(*p*-NO_2)** as well as for dimers with the same substitution, photoinduced ET processes are affected by through-bond interactions [15] and may be considered as bridge-assisted reactions [20]. In the dimer **OEP-Ph-OEP-Ph(*o*-NO_2)**, the k_{et}^{S} value is reduced by three times relative to that of the corresponding monomer **OEP-Ph(*o*-NO_2)**. This reduction may be connected with the competing S–S energy transfer between covalently linked porphyrin macrocycles (rate constants $F^{SS} = (1.9–5.0) \times 10^9$ s^{-1} [8,28]).

The high effective photoinduced ET in all *ortho*-NO_2 substituted compounds is partly due to the influence of steric effects. In this case, the steric hindrance of neighbouring bulky substituents in the β-positions of pyrrole rings and *ortho*-substituents of the *meso*-phenyl spacer significantly restricts internal librations of the phenyl ring about the single C–C bond. Hence, the *ortho*-nitro phenyl octaethylporphyrin moieties are expected to be relatively rigid structures. The molecular mechanics calculations (HyperChem software, release 4, semiempirical AM1 and PM3 methods [21]) for **OEP-Ph(*o*-NO_2)** show that preferable dihedral angles between the porphyrin plane (P), the phenyl plane (Ph) and the nitro group plane (NO_2) are the following: $\alpha(P, Ph) \approx 85 \pm 4°$, $\beta(NO_2, Ph) \approx 80 \pm 4°$ and $\theta(NO_2, P) \approx 60 \pm 5°$. This geometry favours the overlap of molecular orbitals of the porphyrin macrocycle and the NO_2 group and leads to strong electronic coupling, resulting in the effective, direct through-space ET from the locally excited S_1 state to the low-lying CT state [15,20]. In contrast to **OEP-Ph(*o*-NO_2)**, there are no bulky C_2H_5 substituents at the β-pyrrolic positions flanking the *ortho*-nitro phenyl in **TEDM-Ph(*o*-NO_2)** (Fig. 1, compounds **4** and **12**). Because of the reduction of van der Waals spheres overlap for the interacting substituents in the last case [21], it leads to larger amplitudes of the phenyl libration motions about the C–C bond and a corresponding decrease of the electronic coupling term for the ET processes. In fact, the low-effective ET in tetra-*ortho*-phenyl **TPP** [14] may be explained similarly. Nevertheless, in

toluene at 295 K, the rate constant $k_{et}^{S} = 5.0 \times 10^{8}$ s^{-1} for **TEDM-Ph(*o*-NO$_2$)** is higher than that of tetra-*ortho*-phenyl **TPP** ($k_{et}^{S} = 1.5 \times 10^{8}$ s^{-1} in benzene [14]). This fact is explained by different oxidation potentials for **OEP** and **TPP** and will be discussed below.

3.3. Quantitative interpretation of electron transfer processes

In the condensed phase, the hypothetical singlet excited CT state energies may be reasonably estimated according to the well-known formula [2–4]:

$$E_{CT} = e\left(E_{1/2}^{ox} - E_{1/2}^{red}\right) - W, \quad (1)$$

where $E_{1/2}^{ox}$ is the D one-electron oxidation potential, $E_{1/2}^{red}$ is the A one-electron reduction potential, $W = e^2/4\pi\varepsilon_0\varepsilon_{st}r_{DA}$ is the Coulombic interaction energy between the ions at the distance r_{DA} in the D–A pair, where e is the electron charge and ε_0 is the permittivity of free space. On the basis of the W value for Zn-porphyrin–acceptor systems in acetonitrile (the static dielectric constant $\varepsilon_{st} = 35.9$) [29] and the intercenter distance $r_{DA} = 5.7$ Å between the porphyrin and the *ortho*-NO$_2$ group (found for the HyperChem optimised **OEP-Ph(*o*-NO$_2$)** structure) we obtained $W \approx 0.08$ eV in our case. Then using known values of redox potentials (vs. SCE in dimethylformamide, $\varepsilon_{st} = 36.7$) for **OEP** ($E_{1/2}^{ox} = 0.81$ eV [30]), **TPP** ($E_{1/2}^{ox} = 1.08$ eV [27]) and nitro benzene ($E_{1/2}^{red} = -1.08$ eV [27]), we found that $E_{CT} = 1.8$ eV (14 500 cm^{-1}) for **OEP-Ph(*o*-NO$_2$)** and $E_{CT} = 2.1$ eV (16 900 cm^{-1}) for **TPP(*o*-NO$_2$)**.

Accordingly, in **TPP(*o*-NO$_2$)** the predicted CT state is higher by ~ 0.18 eV (1440 cm^{-1}) than the locally excited S_1 state ($E_{S1} = 15\,460$ cm$^{-1} = 1.92$ eV [14]). Hence, the additional deactivation of S_1 state may occur only at the expense of the thermal population of the radical ion pair state or through an increase in the nonradiative transition rate constant caused by mixing with the high-lying CT state [2,31]. In contrast, for **OEP-Ph(*o*-NO$_2$)** the predicted CT state is low-lying by ~ 0.17 eV (1370 cm^{-1}) relative to its S_1 state ($E_{S1} = 15\,870$ cm$^{-1} = 1.97$ eV, in dimethylformamide). Thus, in the latter case, the nonradiative deactivation of the locally excited S_1 state may be due to the direct population of low-lying CT state with a high efficiency. From structural considerations, it follows that $E_{1/2}^{ox}$(**TPP**) > $E_{1/2}^{ox}$(**TEDM**) > $E_{1/2}^{ox}$(**OEP**) which should lead to the intermediate position of the CT state: E_{CT}[**TPP(*o*-NO$_2$)**] > E_{CT}[**TEDM(*o*-NO$_2$)**] > E_{CT}[**OEP(*o*-NO$_2$)**]. Therefore, with the same steric factors resulting in the close values of the electronic coupling terms for **TEDM-Ph(*o*-NO$_2$)** and **TPP(*o*-NO$_2$)** molecules the CT state energy lowering for **TEDM-Ph(*o*-NO$_2$)** may lead to a strengthening of the nonradiative deactivation of the S_1 state in this compound, which is consistent with experimental findings.

At high temperatures, the rate constant k_{et}^{S} for endergonic or moderately exergonic non-adiabatic ET occurring within the 'normal' region is given by the following expressions [15,2,4,31]:

$$k_{et}^{S} = \frac{2\pi}{\hbar}\frac{V^2}{(4\pi\lambda k_B T)^{1/2}}\exp\left(\frac{\Delta G^*}{k_B T}\right), \quad (2)$$

$$\Delta G^* = \frac{(\Delta G^o + \lambda)^2}{4\lambda}, \quad (3)$$

where k_B is Boltzmann's constant, T is the temperature, h is Planck's constant, V is the electronic coupling term between the electronic wavefunctions of the reactant and product states, $\lambda = \lambda_{in} + \lambda_{solv}$ is the Gibbs reorganisation energy determined by the nuclear λ_{in} and solvent λ_{solv} reorganisation energies, ΔG^o is the standard Gibbs energy of the ET reaction and ΔG^* is the Marcus–Gibbs activation energy. For steric reasons, **OEP-Ph(*o*-NO$_2$)** is expected to have a relatively rigid structure. Thus, we may assume that $\lambda_{in} \approx 0.2$ eV, which seems appropriate for porphyrin macrocycles that do not undergo substantial geometry changes upon one-electron redox events [3,4,32]. The λ_{solv} value is often calculated using the formula [4,15,31,32]:

$$\lambda_{solv} = \frac{e^2}{4\pi\varepsilon_0}\left[\frac{1}{2r_D} + \frac{1}{2r_A} - \frac{1}{r_{DA}}\right]\left[\frac{1}{\varepsilon_{op}} - \frac{1}{\varepsilon_{st}}\right], \quad (4)$$

where r_D and r_A are D and A radii, respectively, $\varepsilon_{op} = n^2$ is the optical dielectric constant, n is the refraction index and ε_{st} is the static dielectric constant of the solvent. Based on literature data and the HyperChem optimised structure of **OEP-Ph(*o*-NO$_2$)**,

the following parameters $r_D = 5$ Å [3,29], $r_A = 3.5$ Å and $r_{DA} = 5.7$ Å were obtained. Correspondingly, in acetonitrile the derived value of the outer reorganisation energy is $\lambda_{solv} = 0.5$ eV and the total reorganisation energy is $\lambda = 0.7$ eV.

The standard Gibbs energy of the ET reaction is given by the formula [4,15,31]:

$$\Delta G^o = e\left(E_{ox}^{1/2} - E_{red}^{1/2}\right) - W - E_{S_1}. \quad (5)$$

For **OEP-Ph(*o*-NO$_2$)** this value is equal to $\Delta G^o = -0.16$ eV, and the Marcus–Gibbs activation energy (3) corresponds to the value of $\Delta G^* = 0.1$ eV. Since $|-\Delta G^o| < \lambda$ in this case, the ET process may be assigned to the 'normal' region of the Marcus parabolic dependence, $\log k_{et}^S = f(-\Delta G^o)$ [15].

Based on the picosecond transient absorption measurements of S_1 state decay for **OEP-Ph(*o*-NO$_2$)** in dimethylformamide at 295 K (Table 3), an ET rate constant of $k_{et}^S \approx 2 \times 10^{11}$ s^{-1} was estimated. Thus, using expression (2) and taking into consideration the parameters of λ and ΔG^* obtained as well as the experimental value of k_{et}^S, we estimated the electronic coupling matrix element V to be ~ 190 cm^{-1} in dimethylformamide at 295 K. It is known [33] that ET reactions are non-adiabatic by Landau–Zener criteria if they satisfy the following relationship

$$4\pi^2 V^2 / h\omega (2\lambda k_B T)^{1/2} < 1, \quad (6)$$

where $\omega \approx 100$ cm^{-1} for typical low-frequency solvent motions at 300 K. It follows from the Eq. (6) that at a total reorganisation energy of $\lambda = 0.7$ eV for **OEP-Ph(*o*-NO$_2$)**, the electronic coupling matrix element $V < 130$ cm^{-1}, which does not differ greatly from $V \approx 190$ cm^{-1} obtained using Eq. (2). Thus, assuming realistic errors for λ and ΔG^o estimates one may conclude that at 295 K in polar media the S_1 state quenching in **OEP-Ph(*o*-NO$_2$)** seems to be the limiting case of the non-adiabatic ET with a possible manifestation of some adiabacity effects in strongly polar solvents. Additionally, in the case of $V > 100$ cm^{-1} one may use the adiabaticity parameter of Rips and Jortner [34] in order to evaluate the solvent dynamics influence on the ET rate:

$$K = 4\pi V^2 \tau_L / \hbar \lambda, \quad (7)$$

where τ_L is the longitudinal relaxation time of the solvent (0.4 ps for dimethylformamide). By use of V and λ values for **OEP-Ph(*o*-NO$_2$)** in dimethylformamide at 295 K, we estimated $K \leq 7$. It means that in this case the ET process may be solvent controlled. However, for **OEP-Ph(*o*-NO$_2$)** in non-polar or slightly polar media, as well as for **OEP-Ph(*p*-NO$_2$)** and **OEP-Ph(*m*-NO$_2$)** in both polar and non-polar solvents, the photoinduced ET from porphyrin S_1 states is essentially non-adiabatic.

3.4. Formation and deactivation of locally excited triplet states at room temperature

Table 2 shows that the rate constants k_q^T of T_1 state quenching are lower by 3–4 orders of magnitude relative to the corresponding k_{et}^S values. From the data obtained for **OEP-Ph**, it follows that the rate constant of the nonradiative intersystem crossing $S_1 \rightarrow T_1$ is $r = 5.0 \times 10^7$ s^{-1} and the fluorescence rate constant is $f = 4.5 \times 10^6$ s^{-1}. Thus, in **OEP-Ph(*o*-NO$_2$)** $k_{et}^S = 9.5 \times 10^9$ s$^{-1} \gg r, f$ and a direct population of the T_1 state has a low probability. It manifests itself in the drastic decrease of the quantum yields of both the nonradiative intersystem crossing $S_1 \rightarrow T_1$ (γ_T) and the singlet oxygen generation (γ_Δ) for *ortho*-nitro phenyl substituted octaethylporphyrins (Table 2).

Using phosphorescence spectral data (Fig. 1) we estimated the T_1 state energy for **OEP-Ph(*o*-NO$_2$)** to be $E_T = 1.56$ eV (12 550 cm^{-1}). Accordingly, the excited singlet CT state of the radical ion pair is upper-lying by ~ 0.24 eV relative to that for T_1 state (Fig. 5). Besides, when analysing the temperature dependence of the rate constant k_q^T for **OEP-Ph(*o*-NO$_2$)** in the form of an Arrhenius-type expression [32] we found that the activation energy in the polar toluene–acetone (3:1) mixture corresponds to the value of $\Delta E_a = 0.20$ eV. The D–A pair is certainly more conformationally rigid, the spin-exchange energy is negligible and the spin rephasing between the singlet and triplet radical ion pairs is rather effective with the corresponding rate constants of $k_{13} \approx k_{31} \approx 5.0 \times 10^7$ s^{-1} [4] (Fig. 5). This means that the population of the locally excited T_1 state may take place from the upper-lying triplet radical ion pair state $^3[OEP^+ \cdots NO_2^-]$ or directly from the singlet radical ion pair state $^1[OEP^+ \cdots NO_2^-]$. This reasonable assumption was confirmed by the experimental findings showing that the decrease of the

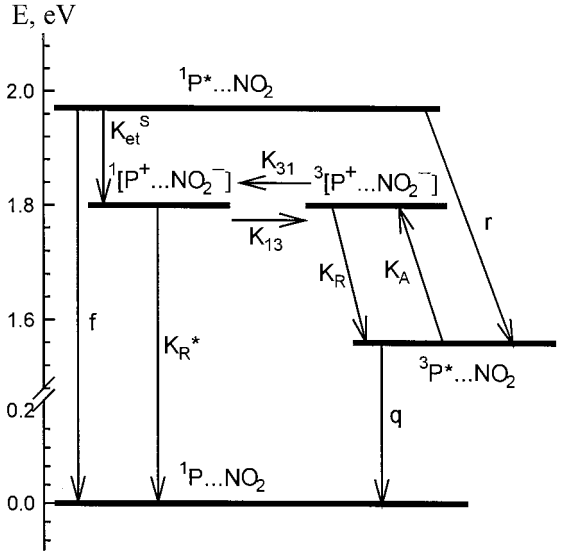

Fig. 5. Schematic energy level diagram for low-lying locally excited singlet ($^1P^* \cdots NO_2$) and triplet ($^3P^* \cdots NO_2$) states, charge-transfer states ($^1[P^+ \cdots NO_2^-]$, $^3[P^+ \cdots NO_2^-]$) and decay pathways of **OEP-Ph(*o*-NO$_2$)** in acetonitrile at 295 K. The rate constants are as follows: *f*, fluorescence; *r*, intersystem crossing from the singlet to the triplet state, $S_1 \rightarrow T_1$; *q*, non-radiative intersystem crossing to the ground state, $T_1 \rightarrow S_0$; k_R^*, charge recombination from the singlet radical ion pair; k_R, charge recombination from the triplet radical ion pair; k_{et}^S, electron transfer from the singlet state; k_{13}, k_{31}, spin rephasing between the singlet and triplet radical ion pairs; k_A, the thermally activated population of the triplet radical ion pair.

fluorescence quantum ($\varphi_F^o/\varphi_F \approx 25$) is not parallel to the decrease of the intersystem crossing quantum yield ($\gamma_T^0/\gamma_T \approx 8$) when going from **OEP-Ph** to **OEP-Ph(*o*-NO$_2$)** in toluene at 295 K. Correspondingly, the non-radiative deactivation of **OEP-Ph(*o*-NO$_2$)** T_1 state may occur via the thermal activation of the radical ion pair states followed by the charge recombination from these states to the ground state:

$$(T_1)\left[^3P \cdots NO_2\right] \underset{K_R}{\overset{K_A}{\rightleftharpoons}} {}^3\left[P^+ \cdots NO_2^-\right] \underset{K_{31}}{\overset{K_{13}}{\rightleftharpoons}} {}^1\left[P^+ \cdots NO_2^-\right] \overset{K_R^*}{\rightarrow} \left[P \cdots NO_2\right](S_0) \qquad (8)$$

(rate constants are defined in Fig. 5). In addition, the τ_T shortening in **OEP-Ph(*o*-NO$_2$)** may also be due to the rise of the intersystem crossing $T_1 \rightarrow S_0$ rate constant caused by a perturbation to the locally excited T_1 state by mixing with upper-lying CT states of the radical ion pair.

4. Conclusions

We have shown that both the S_1 and T_1 states of *meso*-nitro-phenyl octaethylporphyrins and their chemical dimers are quenched relative to the corresponding states of the parent compounds without nitro groups. The direct ET processes are responsible for the observed fluorescence quenching, and ET rate constants are in a reasonable agreement with the predictions of Marcus theory. The population of the locally excited low-lying T_1 state may take place from the upper-lying triplet or singlet CT states. The non-radiative deactivation of the T_1 state may be due to both the thermal activation of the CT states and the rise of the intersystem crossing $T_1 \rightarrow S_0$ rate constant.

With respect to other nitroporphyrins, this study demonstrates that steric hindrance effects and the nature of the linkage between D and A influence on the efficiency and the mechanism of photoinduced ET. Our results also show that the photophysical consequences of the dynamic non-planarity of *meso*-phenyl-substituted octaethylporphyrins in the T_1 state should be included in the quantitative estimation of the quenching efficiency for the corresponding porphyrins with NO_2 groups and more complex arrays on their base.

Acknowledgements

This research was supported by the NFBR of Belarus (Grant No. Ph 96-92). We are grateful to Dr. S. Tikhomirov for picosecond transient absorption measurements of S_1 state decays. We thank also Mr. D. Starukhin for his assistance in temperature experiments on the T_1 state quenching.

References

[1] J. Deisenhofer, O. Epp, K. Miki, R. Huber, H. Michel, J. Mol. Biol. 180 (1989) 385.
[2] M.R. Wasielewski, G.L. Gaines III, M.P. O'Neil, W.A. Svec,

M.P. Niemczyk, L. Prodi, D. Gosztola, in: N. Mataga, T. Okada, H. Masuhara (Eds.), Dynamics and Mechanisms of Photoinduced Transfer and Related Phenomena, Elsevier, New York, 1992, p. 87.
[3] M.R. Wasielewski, Chem. Rev. 92 (1992) 435.
[4] D.D. Fraser, J.R. Bolton, J. Phys. Chem. 98 (1994) 1626.
[5] A. Harriman, J.-P. Sauvage, Chem. Soc. Rev. 25 (1996) 41.
[6] A. Osuka, S. Marumo, N. Mataga, S. Taniguchi, T. Okada, I. Yamazaki, Y. Nishimura, T. Ohno, K. Nozaki, J. Am. Chem. Soc. 118 (1996) 155.
[7] D. Kuciauskas, P.A. Liddell, S.-C. Hung, S. Lin, S. Stone, G.R. Seely, A.L. Moore, T.A. Moore, D. Gust, J. Phys. Chem. B 101 (1997) 429.
[8] E.I. Zenkevich, A.M. Shulga, S.M. Bachilo, U. Rempel, J. von Richthofen, Ch. von Borczyskowski, J. Lumin. 76/77 (1998) 354.
[9] J.L. Sessler, M.R. Johnson, T.-Y. Lin, Tetrahedron 45 (1989) 4784.
[10] S.S. Dvornikov, T.F. Kachura, V.N. Knyukshto, V.A. Kuzmitzkii, K.N. Solov'ev, I.K. Shushkevich, Opt. Spectrosk. 61 (1986) 1228, in Russian.
[11] V.A. Ganzha, G.P. Gurinovich, B.M. Dzhagarov, G.D. Egorova, E.I. Sagun, A.M. Shulga, Zh. Prikl. Spektrosk. 50 (1989) 618, in Russian.
[12] D. Gust, T.A. Moore, D.K. Luttrull, G.R. Seely, E. Bittersmann, R.V. Bensasson, M. Rougee, E.J. Land, F.C. De Schryver, M. Van der Auweraer, Photochem. Photobiol. 51 (1990) 419.
[13] I.K. Shushkevich, V.M. Kopranenkov, S.S. Dvornikov, K.N. Solov'ev, Zh. Prikl. Spektrosk. 46 (1987) 538, in Russian.
[14] A. Harriman, R.G. Hosie, J. Chem. Soc., Faraday Trans. 2 77 (1981) 1695.
[15] R.A. Marcus, Rev. Modern Phys. 65 (1993) 599.
[16] D. Gust, T.A. Moore, A.L. Moore, C. Devados, P.A. Liddell, R. Hermant, R.A. Nieman, L.G. Demanche, J.M. DeGraziano, I. Gouni, J. Am. Chem. Soc. 114 (1992) 3590.
[17] A.V. Chernook, A.M. Shulga, E.I. Zenkevich, U. Rempel, Ch. von Borczyskowski, J. Phys. Chem. 100 (1996) 1918.
[18] J.L. Sessler, V.L. Capuano, A. Harriman, J. Am. Chem. Soc. 115 (1993) 4618.
[19] A. Osuka, N. Tanabe, S. Nakajima, K. Maruyama, J. Chem. Soc., Perkin Trans. 2 (1996) 199.
[20] W.B. Davis, M.R. Wasielewski, M.A. Ratner, J. Phys. Chem. 101 (1997) 6158.
[21] V.N. Knyukshto, E.I. Zenkevich, E.I. Sagun, A.M. Shulga, S.M. Bachilo, Chem. Phys. Lett. 297 (1998) 97.
[22] A.M. Shulga, G.P. Gurinovich, Dokl. Akad. Nauk BSSR 25 (1981) 55, in Russian.
[23] M.J. Gunter, L.N. Mander, J. Org. Chem. 46 (1981) 4792.
[24] R. Young, C.K. Chang, J. Am. Chem. Soc. 107 (1985) 898.
[25] E.I. Zenkevich, E.I. Sagun, V.N. Knyukshto, A.M. Shulga, A.F. Mironov, O.A. Efremova, R. Bonnett, S. Phinda Songca, M. Kassem, J. Photochem. Photobiol. B: Biol. 33 (1996) 171.
[26] S.M. Bachilo, J. Photochem. Photobiol. A: Chem. 91 (1995) 111.
[27] S.L. Murrov, I. Carmichael, G.L. Hug, Handbook of Photochemistry, Marcel Dekker, New York, 1993, p. 269.
[28] E.I. Zenkevich, A.M. Shulga, A.V. Chernook, E.I. Sagun, G.P. Gurinovich, Proc. Indian Acad. Sci., Chem. Sci. 107 (1995) 795.
[29] N. Barboy, J. Feitelson, J. Phys. Chem. 88 (1984) 1065.
[30] J. Fuhrhop, K. Kadish, D. Davis, J. Am. Chem. Soc. 95 (1973) 40.
[31] G.J. Kavarnos, Fundamentals of Photoinduced Electron Transfer, ch. 6, VCH, New York, 1993, p. 287.
[32] A. Harriman, V. Heitz, J.-P. Sauvage, J. Phys. Chem. 97 (1993) 5940.
[33] D.G. Johnson, M.P. Niemczyk, D.V. Minsek, G.P. Wiederrecht, W.A. Swec, G.L. Gaines III, M.R. Wasielewski, J. Am. Chem. Soc. 115 (1993) 5692.
[34] I. Rips, J. Jortner, J. Chem. Phys. 87 (1987) 2090.